Earthquake Engineering, Tenth World Conference © 1992 Balkema, Rotterdam. ISBN 90 5410 060 5

Seismic analysis of underground structures

C. Navarro
Escuela de Ingenieros de Caminos, Ciudad Universitaria, Madrid, Spain

ABSTRACT: This paper extends to other types of structure the simplified methodology proposed by Constantopoulos et al. (1979) for the seismic design of tunnels. As a practical example, a large structure of reinforced concrete, of box shape and totally embedded in soil, is analyzed. The dynamic pressures acting on walls, roof and floor, due to body and surface waves, are considered in the analyses. A set of seismic load combination hypotheses are proposed to account for the different polarization planes of the seismic waves. The influence of neighbouring buildings can be taken into account considering the new soil stress states that they produce.

1 INTRODUCTION

Under seismic conditions, underground structures respond to different seismic waves propagating through soil media. One way to analyze this problem involves three-dimensional finite element analyses using appropriate transmitting boundaries, which allow accurate modelling of the structure and the surrounding soil. These full numerical analyses should be carried out in time domain to account properly for soil non-linear behaviour. However this methodology is expensive when utilized as a design tool of the structure, because it demands long computer time.

Since the pioneering paper of Yeh (1974), in which a simplified analysis for buried pipes subjected to seismic loads was proposed, some attempts have been made to apply those theoretical concepts to the structural design of heavier and more complicated structures, such as underground tunnels and galleries in free-field condition (Constantopoulos et al. (1979 and 1980), Christiano et al. (1983) and Navarro & Samartín (1988)).

In their methodology, Constantopoulos et al. (1979) assumed that tunnels move in a manner similar to that of the surrounding soil, and thus soil-tunnel interaction may be neglected, at least in its traditional sense, because the most tunnel vibration energy is radiated away by soil elastic waves. This method requires only static analyses and accounts very roughly for the difference between tunnel and soil rigidities. They divided the seismic tunnel analysis into two parts: transverse and longitudinal analyses. In the first, a tunnel cross-section is analyzed, considering the soil pressures against tunnel walls, roof and floor caused by the different seismic waves. These pressures are obtained from the stresses in soil in free-field condition, taking into account the changes in the stress distribution around the tunnel originated by its physical presence on soil mass. The types of seismic waves considered in this analysis are: shear and compression waves propagating vertically, and Rayleigh wave components (distorsional and dilatational) travelling horizontally and perpendicularly to the longitudinal axis of the tunnel. Love waves are not considered in this part of the analysis because they are polarized in horizontal planes parallel to the ground surface.

For longitudinal analysis, surface waves propagating parallel to the tunnel axis are considered and the tunnel can be modeled as an elastic beam connected by springs to the far field (Winkler model). Navarro and Samartín (1988) provided an analytical solution for this problem. They considered the tunnel bending analyses, as suggested by Constantopoulos et al. (1979), analyzing the effects on the tunnel caused by the distorsional component of Rayleigh and Love waves, but they incorporated a "push-pull" analysis to account for the influence of the dilatational component of Rayleigh waves, improving that suggested for Constantopoulos et al. (1979). To check the modified analysis, Navarro and Samartín (1988) compared the values so obtained with those recorded in actual earthquakes, observing a high degree of accuracy.

In this paper, the methodology proposed by Constantopoulos et al. (1979) is extended to other types of buried structures. As a practical example, a reinforced concrete large box (12.5*12.5*12.0 meters), protecting diesel tanks, is analyzed seismically. It is founded on intact rock (shear wave velocity v_2 = 2,960 m/s and density ρ_2 = 2.71 tons/m^3) and the walls and the roof are in contact with a granular backfill (v_1 = 300m/s and ρ_1 = 2.06 tons/m^3). The rock material behaviour was supposed elastic, and the variation of the dynamic properties of the granular backfill versus shear strain were taken into account (Hardin and Drnevich (1972)). A structural transverse section is shown in Figure 1.

The seismic excitation consists of two statistically independent accelerograms with a broad frequency content. They are defined at rock/backfill interface level, with a peak acceleration of 0.2g, in both horizontal and vertical directions, and match the response spectra given in the the Regulatory Guide 1.60.

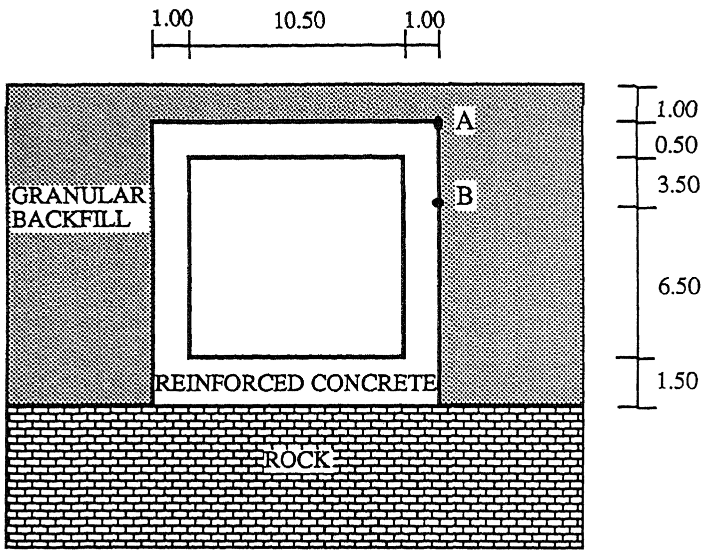

Figure 1. Geometrical definition of the analyzed structure.

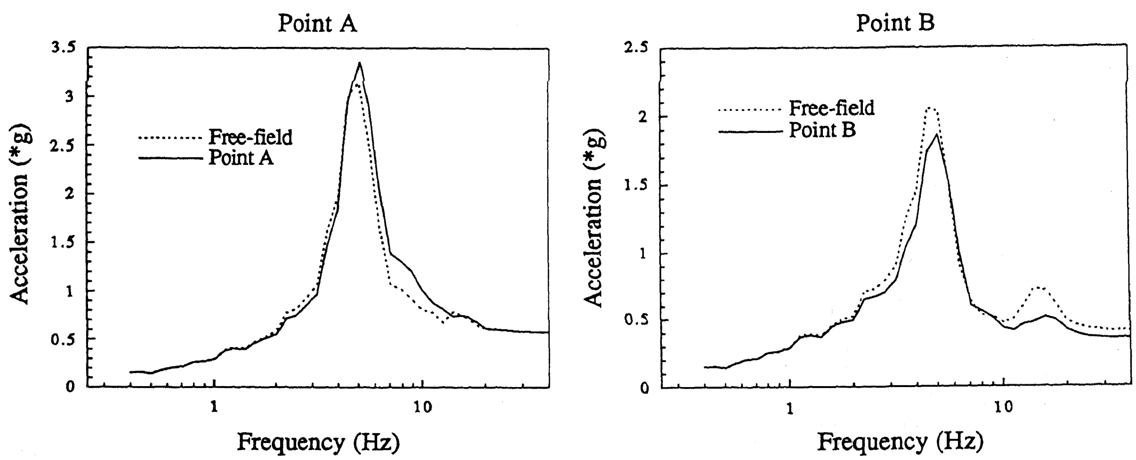

Figure 2. Horizontal response spectra at points A and B (continous line) and at its level in free-field condition (dotted line). Damping ratio 5%.

2 SEISMIC ANALYSIS

2.1 Preliminary SSI studies

To check the importance of soil-structure interaction (SSI) phenomena in these problems, finite element analyses were carried out, in the frequency domain, using the well-known numerical tool FLUSH (Lysmer et al. (1975) which takes into account three-dimensional effects in an approximate manner. The results confirmed that SSI effects were not very important for the case of tunnels (Constantopoulos et al. (1979) and Navarro (1992)), nor for the problem under study (Figure 2). In this figure, the horizontal response spectra at structure points A and B (see Figure 1 for situation), corresponding to horizontal excitation, are compared with those obtained in free-field conditions at the same levels. Maximum spectral ordinates appear for the natural frequency of the soil layer. Differences of about 10% are observed: that for point A is greater than that of free-field, whereas for point B the opposite occurs. For vertical excitation these differences are much less.

2.2 Seismic environment

The determination of a seismic input for buried structures is very complex due to the randomness of direction and the magnitude of the seismic motion, so simplifying and conservative hypotheses should be used to account for the uncertainties of the seismic event. The seismic waves considered are: vertically propagating body (shear and compression), and horizontally propagating Rayleigh waves, all polarized in vertical planes, and Love waves polarized in horizontal planes parallel to the ground surface. The last two waves, normally known as surface waves, have a dispersive character when they propagate through a layered half-space, i.e., wave phase velocity is a function of the frequency of the wave component considered. For the case of Love waves, results of the dispersion equation are shown graphically in Figure 3, for the simple layered half-space considered. For the fundamental frequency range of an earthquake (1-5 Hz), Love wave components propagate to a phase velocity very near to the shear waves velocity of the half-space. A similar conclusion is achieved when treating Rayleigh waves in the same soil system (Ewing et al. (1957)). Fundamental modes of such waves, in the simple layered half-space, show that no changes in soil stresses are observed through layer depth. This means that in free-field conditions, the maximum soil stresses at layer points, due to surface waves, may be computed as:

$$\sigma \text{ (or } \tau) = \frac{v_{particle}}{v_{wave}} * E \text{ (or G)} \quad (1)$$

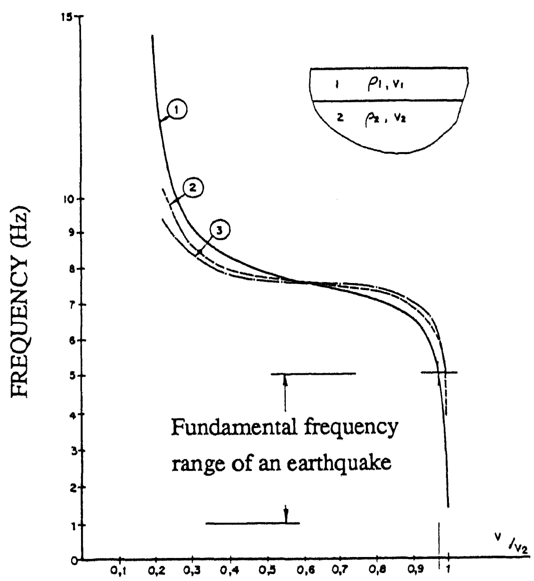

LEGEND:

v = phase velocity of the Love wave component

(1) ρ_1=2.06t/m3,v_1=300m/s,ρ_2=2.5t/m3,v_2=1800m/s

(2) ρ_1=2.06t/m3,v_1=300m/s,ρ_2=2.7t/m3,v_2=2500m/s

(3) ρ_1=2.06t/m3,v_1=300m/s,ρ_2=2.5t/m3,v_2=2960m/s

Figure 3. Dispersion curves for a Love wave propagating through a simple layered half-space.

where $v_{particle}$ is the maximum soil particle velocity, v_{wave} is the wave phase velocity, E and G the elasticity and shear moduli of soil respectively, and σ and τ are the normal and shear stresses in the soil mass due to the seismic wave component. The velocity of soil particles may be obtained from the equation (Newmark et al. (1973)):

$$v_{particle} \text{ (m/s)} = 1.2 \frac{a_{max}}{g} \quad (2)$$

where a_{max} is the soil peak acceleration. In the case of Rayleigh waves, the stress state induced in the soil consists of a normal stress, acting on vertical planes, together with a shear stress component. The first can be computed using Eq. (1) and considering a modulus E accordingly with the shear deformation. The second stress component may be assumed as 10% of the previous one, for a layer depth below 5% of the Rayleigh wave length (Wolf (1985)).

The soil stresses caused by vertically propagating body waves may be calculated by means of the computer program SHAKE (Schnabel et al. (1975)) or by using the simplified method suggested by Seed and Idriss (1971) to evaluate soil shear stresses caused by the vertical propagation of shear waves. The author has checked that the approximate expression given by Seed and Idriss (1971) can also be used for vertically propagating compression waves, considering the same coefficients but introducing the vertical acceleration at ground level.

2.3 Seismic soil pressures

Once the soil stresses in free-field, caused by each basic wave type, are known, soil pressure distributions can be computed using a static finite element mesh in which the structure and a part of the surrounding soil are modeled, as suggested by Constantopoulos et al. (1979). In this manner, pressure concentration effects at structure corners, caused by the structure and soil stiffness differences, can be taken into account. Thus the normal and shear stress distribution, acting on the vertical wall zone and at the middle structure width, due to shear, compression and Rayleigh waves are obtained (Figure 4).

This figure presents some ponits of interest. First of all, the pressure distributions do not follow the Mononobe-Okabe theory (Seed and Whitman (1970)) of seismic earth thrust predictions. This is due to the wall flexibility; the theory is not applicable to this type of structure. The shear stress values due to vertical propagation of shear wave are much higher than those obtained from either Rayleigh or compression waves. Note that the first reach a maximum of about 10.5 tons/m^2 whereas the second values between 0 and 2 tons/m^2. Although the shear stress values would be limited by soil-wall friction phenomena, the axial forces at the wall/floor level will be governed by shear wave propagation. The normal stresses acting on the wall due to Rayleigh and compression waves are very similar, and in practice can be assumed as constant along the wall. Those caused by shear wave present a minimum value about the middle of the wall and maximum values

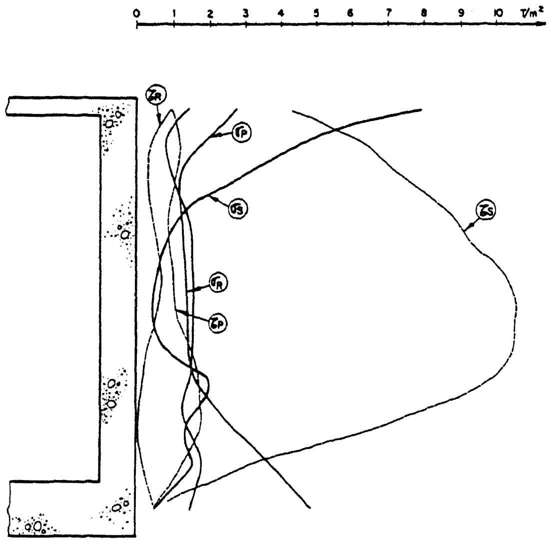

LEGEND:
σ = normal stress
τ = shear stress
Subscripts P, S and R represent respectively Shear, Compression and Rayleigh waves

Figure 4. Stress distribution around the wall caused by different seismic waves. (Vertical plane)

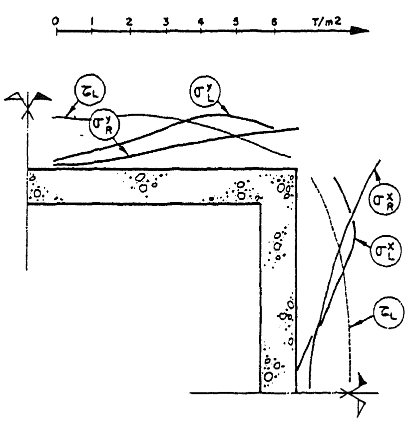

LEGEND:
σ = normal stress
τ = shear stress
Subscripts L and R represent respectively Love and Rayleigh waves

Figure 5. Stress distribution around walls corner caused by different seismic waves. (Horizontal plane)

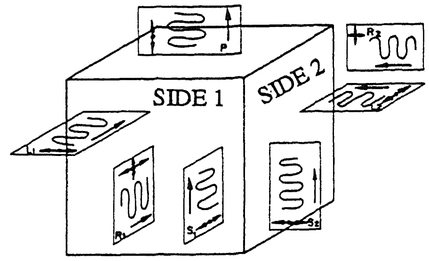

LEGEND:
Type of movement adquired by soil particles
S - Shear wave
P - Compression wave
R - Rayleigh wave
L - Love wave
Direction of wave propagation

Figure 6. Seismic waves considered and their supposed polarization planes.

at the wall corners, as a consequence of the stress concentration effect mentioned. The shear force and bending moment in the wall seem to be due to either compression or Rayleigh waves. However axial force and bending moment at wall/floor and wall/roof rather appear to be due to shear waves.

Figure 5 shows the stress distribution across a quarter of a horizontal cross-section, at the middle of structure height. Only Rayleigh and Love wave effects are considered in this figure. The normal stresses reach minimum values at the middle of the wall, and shear stresses due to Love waves can be considered as constant.

Accordingly to the polarized planes of each basic wave type, shown in Figure 6, and to the terms of the Regulatory Guide 1.92, the following seismic loads combinations apply:

a) $S_1 - S_2 - P$	b) $S_1 - R_2$
c) $S_1 - L_1 - P$	d) $S_2 - R_1$
e) $L_2 - S_2 - P$	f) $R_1 - L_1$
g) $L_1 - L_2 - P$	h) $R_2 - L_2$

where S, P, R and L represent respectively any internal load or bending moment due to a pressure distribution corresponding to shear, compression, Rayleigh and Love waves, and the subscripts give the structural sides where the seismic pressures are supposed acting. The design loads should be computed as the envelope of those calculated in each combination hypothesis.

2.4 Influence of neighbouring buildings

When massive building are founded near the considered structure, this methodology does not necessarily lead to conservative design values. Recent works (Gómez-Massó and Atalla (1984) and Navarro (1992)) on this last subject prove that the influence of buildings can greatly alter the stress states generated in soil mass regarding those obtained in free-field situation.

So, for the case of a building (8,000 tons) founded at surface (Figure 7(a)) on a soil system of the same dynamic properties and seismic input as said before, Figure 8(a) shows the stress state, generated into the soil, at different distances from the building edge and in the middle of the layer depth, for horizontal excitation. For approximately 30 meters from the building edge, the influence of the building has disappeared. For vertical excitation the influence decreases much faster.

Figure 7(b) shows another case very common in Nuclear Power Plants facilities: a Reactor building of 120,000 tons weight and 60 m diameter, founded on a half-space, with a shear wave velocity of about 1,100 m/s. The building is surrounded by a granular backfill layer 10 m deep, whose dynamic properties are those proposed by Hardin and Drnevich (1972). The horizontal seismic input is an accelerogram of peak acceleration 0.12g, defined at backfill surface, and matching the response spectrum of the Regulatory Guide 1.60. The dependence of the stress state on distance from the wall, at an intermediate layer depth, is shown in Figure 8(b). At a distance of about 30 meters, the influence of the building seems to disappear. However, this is not exactly true because Navarro (1992) has shown that an interference phenomena between Rayleigh waves, propagating horizontally through the backfill layer and away from the building wall, and vertical travelling shear waves, occurs at more than 30 m from the wall. To illustrate this, Figure 9 shows the response spectra, for a damping ratio of 5%, obtained at different points of the layer. At about 40 m, the spectral ordinates are greater than those obtained in free-field. The distance at which this takes place is a function of the wave length of the Rayleigh wave (Navarro (1992)).

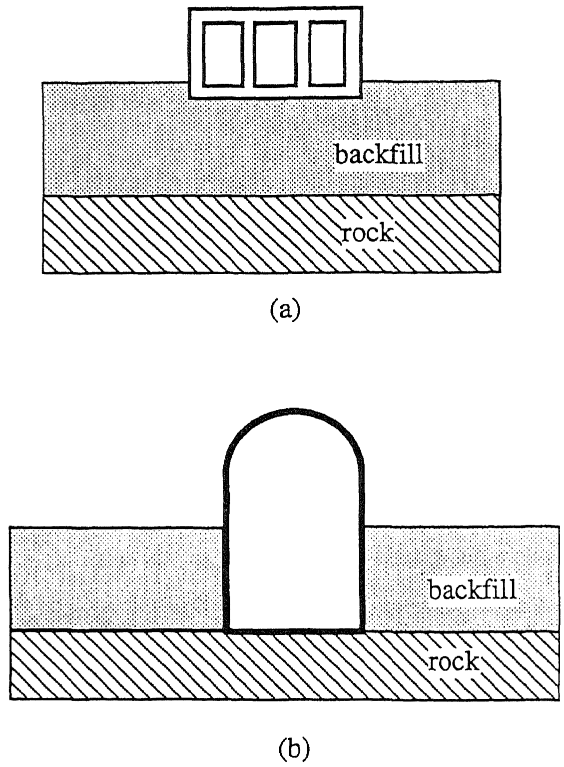

Figure 7. Different structural systems

3 CONCLUSIONS

This paper outlines a simplified methodology for the design of large structures other than tunnels and galleries. It is an extension of that proposed by Constantopoulos et al. (1979).

Some recommendations are made about the choice of Rayleigh and Love wave velocities to be used in the analysis. This greatly simplifies the consideration of the effects of the seismic waves.

Combination criteria, attending to the different polarization planes of the seismic waves involved, are provided.

Particular attention should be given when massive buildings are near the buried structure because then some of the results of the simplified methodology may not be conservative.

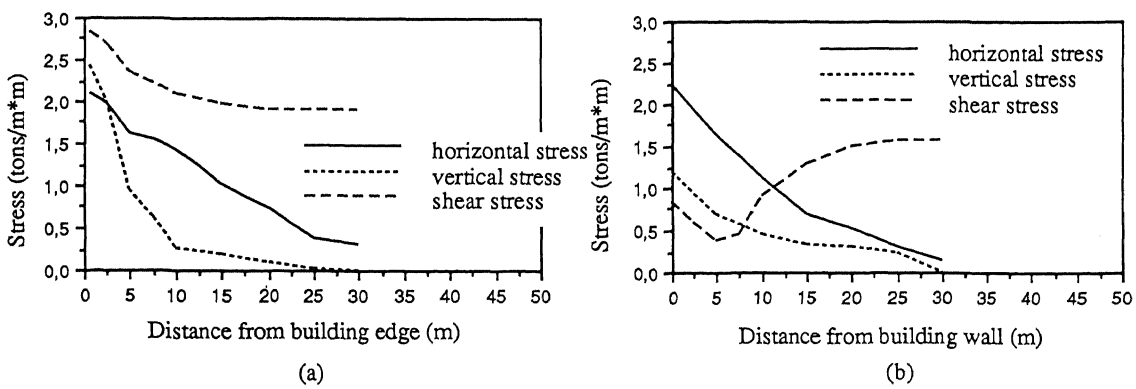

Figure 8. Stress states

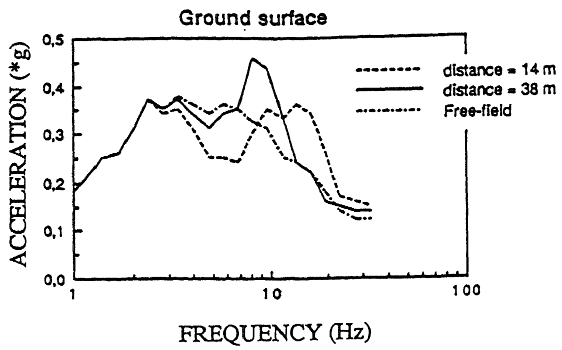

(a)

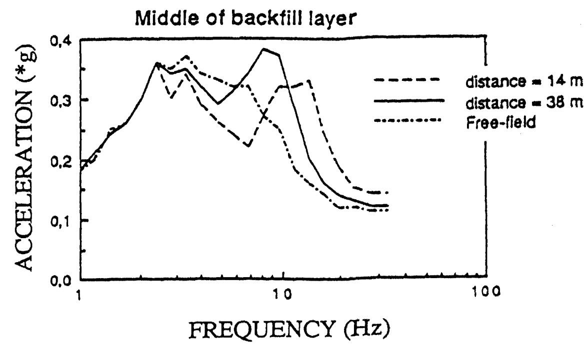

(b)

Figure 9. Response spectra for a damping ratio of 5% at different distances

REFERENCES

Constantopoulos, I.V. et al. 1979. Dynamic analysis of tunnels. Proc. 3rd. Int. Conf. Num. Meth. Geomech..

Constantopoulos, I.V. et al. 1980. Seismic analysis of buried tunnels. Proc. 7th. World Con. Earthquake Engng.

Christiano, P.P. et al. 1983. Response of buried tunnels to earthquake excitation. Trans. 7th Int. Conf. Struct. Mech. Reactor Tech., Vol. K: 287-294.

Ewing, W. M. et al. 1957. Elastic waves in layered media. Prentice-Hall.

Gómez-Massó, A. & I. Atalla 1984. Finite element versus simplified methods in the seismic analysis of underground structures. Earthquake Engng. Struct. Dyn. 12: 347-367.

Hardin, B.O. & V.P. Drnevich 1972. Shear modulus and damping in soils: design equations and curves. J. Soil Mech. Found. Div. ASCE 98: 603-624.

Lysmer, J. et al. 1975. FLUSH, a computer program for approximate 3D analysis of soil-structure interaction problems. Rep. EERC 75-30.

Navarro, C. & Samartín, A. 1988. Simplified longitudinal analysis of buried tunnels. Software for Engng. Workstations 4: 3-10.

Navarro, C. 1992. Effect of adjoining structures on seismic response of tunnels. Int. J. Num. Anal. Meth. Geomech. (in press).

Newmark, N.M. et al. 1973. Seismic design spectra for Nuclear Power Plants. J. Power Div. ASCE 99.

Schnabel, P.B. et al. 1975. SHAKE- A computer program for earthquake response analysis of horizontally latered sites. Rep. EERC 72-12.

Seed, H.B. & Idriss 1971. Simplified procedure for evaluating soil liquefaction potential. J. Soil Mech. Found. Div., ASCE 97:1249-1273.

Sedd, H.B. & Whitman, R.V. 1970. Design of earth retaining structures for dynamic loads. Lateral stresses in the ground & design of earth retaining structures.ASCE.

USNRC. Regulatory Guide 1.60. Design response spec-tra for seismic design of Nuclear Power Plants.

USNRC. Regulatory Guide 1.92. Combining modal res-ponses and spatial components in seismic response analysis.

Yeh, G. C. K. 1974. Seismic analysis of slender buried beams. Bul. Seis. Soc. America 64: 1551-1562.

Wolf, J.P. 1985. Dynamic soil-structure interaction. Prentice-Hall.